THIRD SEMI-ANNUAL REPORT

June 1, 1965 to November 30, 1965

Under NASA Grant NsG-601

on

"OSCILLATORY COMBUSTION IN ROCKETS"

N66-23828

FACILITY FORM 602

(ACCESSION NUMBER)

(PAGES)

CR-71895

(NASA CR OR TMX OR AD NUMBER)

(THRU)

(CODE)

33

(CATEGORY)

Prepared By

R. Goluba
H. Hiroyasu
J. Manrique
J. Ricart-Lowe
R. Sowls
D. Wendland

Supervisors

Professor G.L. Borman

Professor P. S. Myers

Professor O.A. Uyehara

Mechanical Engineering Department
University of Wisconsin
Madison, Wisconsin 53706

GPO PRICE $ _____

CFSTI PRICE(S) $ _____

Hard copy (HC) ____3.00____

Microfiche (MF) ____.75____

ff 653 July 65

TABLE OF CONTENTS

Third Semi-Annual Report
To The National Aeronautics and Space Administration
On Research Grant NsG-601
June 1, 1965 - November 30, 1965

I. INTRODUCTION

The research being conducted under this grant is aimed at obtaining

a more fundamental understanding of some of the aspects of oscillatory com-

bustion. There are three separate, but related, investigations being conducted

under this grant.

The first investigation deals with the vaporization of liquid under con-

ditions where the liquid may pass through its critical point. Work has con-

tinued on developing the vaporization theory, and building an experimental

apparatus for measuring temperatures and vaporization rates of suspended drops.

In addition to these existing projects, another project was begun to design and

build the apparatus necessary to study the vaporization of falling drops.

The second investigation deals with heat transfer from a gas to a solid

surface when the gas is undergoing large pressure oscillations. The first

project, which utilizes a cylinder and piston to obtain pressure oscillations

in a no-flow closed system, progressed to the data-taking phase during the

reporting period. In the second project work was continued on designing and

constructing the apparatus for the project which uses a siren to obtain pressure

oscillations in a flowing gas.

The third investigation deals with size and velocity distribution

measurements in sprays. While work was continued by J. Groeneweg (now at

NASA - Lewis) on analysis of the velocity-size data obtained during the last reporting period, no further projects dealing with sprays were begun. However, a short-term project to test the feasibility of using a laser as a light source for spray pictures was carried out. A report on this study is attached to this report.

There has been a shortage of graduate students interested in and available for this project. Since it was felt that, of the three projects, the drop vaporization in the region of the critical state was the most urgent, it was decided to momentarily terminate the spray studies and to use the manpower from this study on the vaporization studies. Accordingly, for the last two months, Dr. Hiroyasu and Mr. Sowls have spent their time on theoretical work and on possible designs to study falling droplets under conditions near the critical state. It is planned to reactivate the drop experiments as soon as manpower is available.

III. VAPORIZATION IN THE REGION OF THE CRITICAL STATE

A. DROPLET VAPORIZATION THEORY

A start was made on revising the drop vaporization theory of Priem,

et al, to fit conditions near the critical point. The corrections are based

primarily on removing the assumption of an ideal gas. The following analysis

shows some of the details involved in correcting the mass transfer equation.

Aside from these corrections, all of the properties such as vapor pressure,

specific heats, etc., must be calculated to include the effect of pressure.

Correction of the diffusion coefficient for non-ideality may or may not be in-

cluded in the values reported in the literature (see p. 569, Eqs. 18.4-16,

18.4-17, Transport Phenomena, Bird, et al).

The molar flux relative to stationary coordinates may be written

(see p. 502, Transport Phenomena)

$$\vec{N}_A = X_A (\vec{N}_A + \vec{N}_B) - CD_{AB} \nabla X_A \tag{1}$$

where

$\vec{N}_A$ = molar flux of species A

$\vec{N}_B$ = molar flux of species B

$C = C_A + C_B$ - molar density of solution

C_A = molar concentration of A

X_A = mole fraction of A

D_{AB} = diffusion coefficient

Eq. (1) shows that the diffusion flux $\vec{N}_A$ relative to stationary coordinates

is the resultant of two vector quantities where the vector $X_A (\vec{N}_A + \vec{N}_B)$

is the molar flux of A resulting from the bulk motion of the fluid.

If we assume $N_B = 0$; solving for N_A, we get

$$N_A = -\frac{CD_{AB}}{1-X_A}\frac{dX_A}{dr} \tag{2}$$

$$C = \frac{\tilde{P}_T}{RT}, \quad X_A = \frac{\dfrac{P_A}{Z_A}}{\tilde{P}_T} \tag{3}$$

where

$$\tilde{P}_T = \frac{P_A}{Z_A} + \frac{P_B}{Z_B}$$

$$P_T = P_A + P_B$$

P_A and P_B = partial pressures

and Z_A and Z_B = compressibility factors.

If we assume $Z_B = 1$

$$N_A = \frac{\tilde{P}_T D_{AB}/(RT)}{1 - P_A/(Z_A\tilde{P}_T)} \quad \frac{d}{dr}\left[P_A/(Z_A\tilde{P}_T)\right] \tag{4}$$

$$\frac{d}{dr}\left[\frac{\frac{P_A}{Z_A}}{\tilde{P}_T}\right] = \frac{d}{dr}\left[\frac{\frac{P_A}{Z_A}}{\frac{P_A}{Z_A} + P_B}\right] = \frac{1}{\tilde{P}_T}\left[\bar{A}\ \frac{dP_A}{dr} + \bar{B}\ \frac{dX_A}{dr}\right]$$

where

$$\bar{A} = \frac{1}{Z_A} - \frac{P_A}{Z_A^2\left[\frac{P_A}{Z_A} + P_B\right]} + \frac{P_A Z_A}{Z_A^2\left[\frac{P_A}{Z_A} + P_B\right]} = \frac{P_A + P_B}{P_A + P_B Z_A}$$

$$\tag{5}$$

$$\bar{B} = \frac{P_A}{Z_A^2} - \frac{P_A^2}{Z_A^3\left[\frac{P_A}{Z_A} + P_B\right]} = \frac{P_A P_B}{Z_A P_A + P_B Z_A}$$

Therefore,

$$N_A = -\frac{\frac{1}{RT} D_{AB}}{\tilde{P}_T - \frac{P_A}{Z_A}} \cdot \frac{1}{\tilde{P}_T}\left[\bar{A}\ \frac{dP_A}{dr} + \bar{B}\ \frac{dZ_A}{dr}\right]$$

$$= -\frac{D_{AB}}{RT}\ \frac{P_A + P_B Z_A}{P_B Z_A}\left[\frac{P_A + P_B}{P_A + P_B Z_A}\ \frac{dP_A}{dr} + \frac{P_A P_B}{Z_A(P_A + P_B Z_A)}\ \frac{dZ_A}{dr}\right] \tag{6}$$

$$= -\frac{D_{AB}}{RT}\left[\frac{P_T}{Z_A(P_T - P_A)}\ \frac{dP_A}{dr} + \frac{P_A}{Z_A^2}\ \frac{dZ_A}{dr}\right]$$

By a shell balance, for a spherical droplet,

$$r^2 N_{Ar} = r_s^2 N_{Ar_s} \tag{7}$$

Boundary conditions

$$r = r_s \quad : \quad P_A = P_f \qquad Z_A = Z_{Af}$$

$$r = r_s + B \quad : \quad P_A = 0 \qquad Z_A = 1$$

$$N_{Ar_s} \frac{r_s^2}{r^2} = - \frac{D_{AB}}{RT} \left[\frac{P_T}{Z_A(P_T - P_A)} \frac{dP_A}{dr} + \frac{P_A}{Z_A^2} \frac{dZ_A}{dr} \right]$$

(8)

$$N_{Ar_s} r_s^2 \int_{r_s}^{r_s+B} \frac{dr}{r^2} = - \frac{D_{AB}}{RT_m} \left[\int_{P_f}^{0} \frac{1}{Z_A} \cdot \frac{P_T \, dP_A}{(P_T - P_A)} + \int_{Z_{Af}}^{1} P_A \cdot \frac{dZ_A}{Z_A^2} \right]$$

by mean value theorem for integrals

$$N_{Ar_s} \frac{r_s B}{r_s + B} = - \frac{P_T D_{AB}}{RT_m} \left[\frac{1}{Z_{Am}} \ln \left[\frac{P_T - P_f}{P_T} \right] + \frac{P_{Am}}{P_T} \left[\frac{1}{Z_{Af}} - 1 \right] \right]$$

(9)

$$N_{Ar_s} = \frac{D_{AB} P_T}{RT_m} \left[\frac{1}{r_s} + \frac{1}{B} \right] \left[\frac{1}{Z_{Am}} \ln \left(\frac{P_T}{P_T - P_f} \right) + \frac{P_{Am}}{P_T} \left[1 - \frac{1}{Z_{Af}} \right] \right]$$

$$W_A = A_0 \cdot N_{Ar_s} \cdot M_A$$

(10)

$$= \frac{D_{AB} M_A}{RT_m} A_0 \left[\frac{1}{r_s} + \frac{1}{B} \right] P_f \cdot \bar{\alpha}$$

where

$$\bar{\alpha} = \frac{P_T}{P_f} \left[\frac{1}{Z_{Am}} \ln\left(\frac{P_T}{P_T - P_f}\right) + \frac{P_{Am}}{P_T} \left(1 - \frac{1}{Z_{Am}}\right) \right]$$

$$= \frac{\alpha}{Z_{Am}} + \frac{P_{Am}}{P_f} \left[1 - \frac{1}{Z_{Af}}\right]$$

and $\quad \alpha = \frac{P_T}{P_f} \ln \frac{P_T}{P_T - P_f}$

The range of the mean values is given by:

$Z_{Af} = Z_A$ at liquid surface $\quad 0 < Z_{Af} < 1$

$Z_{Am} = $ some mean Z_A in film $\quad Z_{Af} < Z_{Am} < 1 ; \quad \dfrac{Z_{Af} + 1}{2}$

$P_{Am} = $ some mean P_A in film $\quad 0 < P_{Am} < P_f ; \quad \dfrac{P_f}{2}$

$T_m = $ some mean T in film $\quad T_L < T_m < T_A ; \quad \dfrac{T_A + T_L}{2}$

$$P_f < P_c$$

The above estimates for $\bar{\alpha}$ could, of course, be refined by a more exact integration of Eq. 8. However, one should keep in mind that many assumptions are already included in Eq. 8 so that a more exact integration may not yield much more precise results.

Turning next to the calculation of the partial pressure at the liquid surface, P_f, we must correct the vapor pressure for the effect of total pressure.

Keenan shows the effect of pressure on vapor pressure by the following thought experiment where a porous column (porous to vapor, but not to liquid) is filled with liquid and the entire container filled with the vapor. At point S at the top of the liquid, we have the usual definition of vapor pressure, P_{SA} , where P_{SA} is the vapor pressure on would look up according to temperature. However, at point A at the bottom of the container, there must be equilibrium between the vapor and the liquid inside the tube with both being at the same temperature as S, but at different pressures. For a single phase at constant temperature
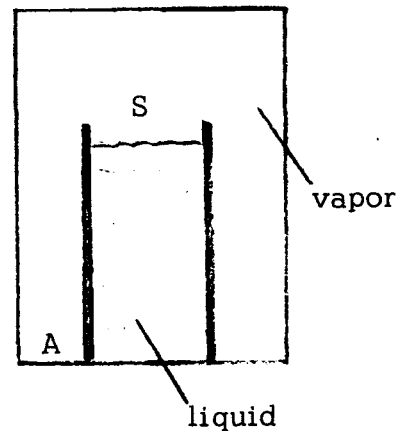
$$dG = -Vdp \tag{11}$$

or for the liquid

$$\int_S^A dG = \int_S^A V' \, dp'$$

For the vapor

$$\int_S^A dG = \int_S^A -V'' \, dp''$$

and since they are in equilibrium, the two integrals must be equal, or

$$\int_S^A V'' \, dp'' = \int_S^A V' \, dp \tag{12}$$

Using $PV = ZRT$ for the vapor

$$\int_{P_S}^{P_A} V'' \, dp'' = \int_{P_S}^{P_A} \frac{Z_A RT}{P_A} \, dP_A = RT \int_{P_S}^{P_A} Z_A \frac{dP_A}{P_A} = \int_{P_S}^{P_T} V_{LA} \, dP \tag{13}$$

V_{LA} is the volume of the liquid and could be expressed via the ω charts

of Watson in terms of reduced pressure and temperature; likewise the integral

for the vapor could be put in terms of the reduced temperature and pressure.

The value of P_A obtained from Eq. 13 is the value to be used at the liquid

surface in the mass transfer computations.

In order to calculate vaporization histories from the above revised

theory, it is necessary to obtain expressions for Z (Tr, Pr) which can be used

in the computer. We are thus presently working on a curve fitting procedure

for Z. Expressions must also be obtained for the corrected partial pressure

(Eq. 13) and for the other properties. It is planned to obtain these property

equations and then incorporate them with the above theory. A computer pro-

gram for calculating vaporization histories will then be written in order to

evaluate the changes brought about by the revised theory.

In addition to the above empirical approach, work has just begun on a

basic approach using the fundamental equations of change. The model will

assume complete spherical symmetry (i.e., neglect all convective terms).

Although such an analysis has a very restricted practical utility, it should

help in clarifying the effects of non-ideality and the effects of using various

mean property values.

III. VAPORIZATION IN THE REGION OF THE CRITICAL STATE

B. SUSPENDED DROP EXPERIMENTS

In this experiment it is planned to flow heated high-pressure air over a suspended drop. Provision is made for continually feeding new liquid to the drop at a known rate and temperature. The drop size, mass flow feed rate, and drop temperature are to be measured.

The general design of the apparatus was shown in the previous report. Work continued during this period on making and checking out final design drawings for the air nozzle and air feed, the optical windows, and the probe. Some modifications in the design of the nozzle for the high pressure test section were necessary in order to allow longer running times (on the order of 1/2 hour), and to cut down on the necessary capacity of the air heater. It is estimated that fabrication of the test section should be completed by the end of February.

Design work on a conventional type of air heater was begun. The heater design is shown in Fig. 1. The probe and mass flow measuring device still remains as a problem which has not been completely solved. The current design would replace the capillary measuring tube with a positive displacement system. In the next six months, it is hoped to assemble the apparatus and start the preliminary calibration of the same. This calibration will consist of running experiments at low pressures to see how they relate to similar experiments done by Priem and Borman in the past. It is hoped that similar

Air Out

High Pressure
Electric Connector

Air In

6 in. ID pipe
71/2 in. OD
carbon steel

Calrod
heater

Iron
Beads

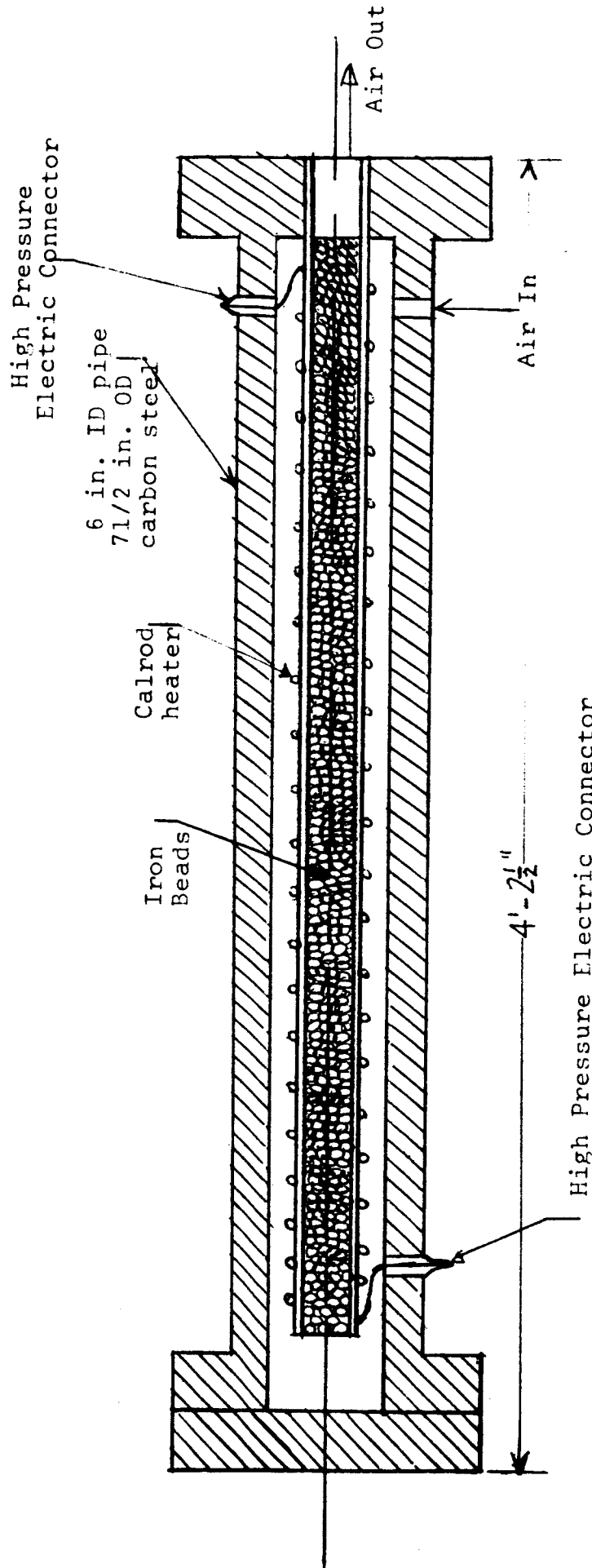$4' - 2\frac{1}{2}''$

High Pressure Electric Connector

Fig. 1

Proposed Design of Low Temperature Heater

results will be obtained. After this stage is complete, then it is intended to run experiments at increasingly high pressures until the critical conditions are approached. This stage will probably be reached in the latter half of 1966. It is not clear whether or not it will be possible to study a hung droplet at the critical temperature since the surface tension of liquids decreases steadily with increasing temperature. It is in this area that problems are expected to develop. The upper limit in temperature for drop hanging purposes is uncertain at this time.

A series of simple experiments with Freon-113 are planned to determine its drop hanging characteristics at atmospheric pressures and temperatures. Freon-113 will be used because it is a liquid under these conditions, while Freon-13 is not. It is expected to obtain useful information out of this experiment in the sense that it will be of great help in the designing of the fuel controls of the experimental setup.

In order to be able to take the fuel to the critical temperature, a porous sphere arrangement may be indicated. The porous sphere, however, will be much more difficult to analyze and there may be some doubt as to the meaning of the results thereby obtained.

III.   VAPORIZATION IN THE REGION OF THE CRITICAL STATE

C.   FALLING DROP EXPERIMENTS

It would be desirable to know qualitatively and quantitatively what can be expected to happen when a liquid is sprayed into an atmosphere at a pressure and temperature greater than the critical temperature and critical pressure of the liquid. Because of the number of droplets involved and because of possible interactions between droplets in sprays, the direct experimental study of what happens to any given drop in a spray appears to be an exceedingly complex task. Since its inception approximately 2 - 3 months ago, the goal of this project has been to devise experimental techniques with which to study the behavior of single drops of a suitable liquid injected into a gas whose temperature and pressure are greater respectively than the critical temperature and the critical pressure of the liquid material. The results that are desired from the experiment are: (1) qualitative knowledge of anything unusual or unexpected that may happen to a vaporizing droplet as it approaches its critical temperature; and (2) experimental verification of methods of calculating the motion, mass, and temperature histories of droplets vaporizing in an atmosphere where the temperature and pressure are greater than the critical temperature and the critical pressure of the liquid.

It is proposed to study a droplet which is not disturbed by being suspended from a support. The experiment is to be based on obtaining the motion, mass, and temperature histories of single drops falling free through a stagnant

atmosphere of temperature and pressure greater than the respective critical properties of the liquid. The apparatus must provide the high-temperature, high-pressure atmosphere a means of forming and releasing a single drop of controlled initial size and temperature into the hot gas, and means of measuring or inferring the motion, mass, and temperature histories of the drop.

Two general methods have been considered for obtaining the desired histories. These are:

1. Construct the histories for a given initial drop size and temperature by (a) measuring the time to fall a given distance and the size (radius and mass), velocity, and temperature at the end of the fall, and (b) repeating the measurements for various distances.

2. Determine the position and radius history of each drop by photographing it a number of times in its fall and infer as well as possible its mass and temperature history.

Both of these methods would use photography for determining position and radius histories and it is felt that commercially available cameras and light sources can be adapted to either technique. The most serious photographic problem appears to be the design and construction of test chamber windows which will withstand the high pressures and high temperatures and still allow high quality photography. Several tentative window designs are under consideration.

Experimental measurement of the mass and temperature histories of a drop pose difficult problems with either of the above general methods.

Although the question of the direct applicability of any commercially available apparatus to either droplet mass or droplet temperature history measurements is still open, no easy or sure solution has yet been uncovered for either quantity. The following ideas and suggestions of possible methods for measuring mass and temperature histories of droplets have grown out of discussions held with everyone directly concerned with this project and with other interested parties.

Two possibilities for measuring the mass history that might be adaptable to general method I, above, are:

1. Terminate the motion and vaporization of the drop and weigh it on an extremely sensitive balance. The details of this idea have not been completely worked out.

2. Impact the drop on a special instrument which will measure the momentum of the drop carried when it struck. The mass of the drop can then be determined because the velocity with which the drop struck was measured photographically.

Because of the very small mass of a drop, either of these methods must use very delicate apparatus if they are to succeed.

A possible third method involves catching the drop in a known quantity of gas —i.e., letting them mix and determining the mass of the drop by gas chromatography.

The mass of a drop for general method II above might be inferred at points along its path by dividing the test chamber into a number of connected

cells that can be quickly isolated from one another after the passage of the drop. Then the vapor content of each cell might be determined by gas chromatography or by other means. Then knowing the initial mass of the drop, and how much vapor it has left behind, its mass can be calculated for positions corresponding to the exit from each cell. The potential value of this method requires further exploring and it depends to a considerable extent on the gaseous and liquid materials to be investigated. It also presents construction problems with regard to isolating the cells until the samples are withdrawn and of withdrawing samples so as not to cause gas to flow from one cell to the other. It would seem that data reduction would be quite tedious and expensive.

Thus far, three potential experimental methods for determining droplet temperature have been considered. Two involve optical techniques and, if workable, might be applied to general method II above. These are:

1. To somehow measure an optical property of the drop that is temperature dependent while the drop is in flight and to relate the value of the property to the temperature. At the moment, this does not seem feasible.

2. To measure the intensity of infared radiation emitted from the drop using a rapid response infared radiometer such as a gold-doped germanium cell. This technique would require considerable preliminary work in correlating the intensity of radiation with the temperature of the droplet and, indeed, it may not work at all.

3. This method would be applicable only to general method I above. It consists of impacting a drop on the face of a thin film thermo-couple which is mounted on a heat sink. The temperature of the heat sink will be varied until there is no change in the thermocouple read-ing when the droplet strikes the junction. This seems to be the most workable of the suggested methods of determining droplet temperature.

From the above ideas, the method of building up a history of a given initial size and initial temperature of droplet has been selected for the initial attempt. Some testing will be done before the methods of measuring the mass and the temperature of droplets are selected.

A method for obtaining the position of a droplet as a function of time, and possibly the radius as well, is also to be tested. The method involves letting the drop fall through collimated light which is directed at a transmission grating. A photoelectric cell is situated behind the transmission grating. Each time the shadow of the drop falls on an opaque part of the grating, the photo-electric cell will give a no signal indication. It is hoped that the radius of the droplet can be determined from the size of the signal of the photoelectric tube while its position will be given by the number of no signal indications up to a given time.

While the past few months have been spent primarily developing ideas with which to attack the problem, the next several months will be devoted to the design, construction, acquisition, and testing of apparatus.

The first apparatus to be constructed will be a test chamber and associated drop forming apparatus. The apparatus will be designed to form a single drop of liquid carbon dioxide, at a controlled low temperature, and to release this drop at will to fall into a high temperature atmosphere of nitrogen. Windows will be provided at the top of the test chamber and at the bottom, so that the initial droplet size and its size after falling through a known distance can be determined using a shadow photographic technique. The distance between the top and bottom windows will be varied by adding segments to the test chamber between them. The light source for each camera will be triggered by the signal from a photoelectric cell when a droplet falls through a small light beam that is crossing the camera axis. The time required for the droplet to fall from one camera axis to the other will be determined by using the photoelectric cell signals to make and break an electrical connection between an electronic counter and an electronic oscillator of a suitable frequency. It is estimated that the design and construction of the above described test chamber and drop forming apparatus will require two to three months. Although this apparatus is being designed with gaseous N_2 and liquid CO_2 in mind, it will also be suitable for other liquids, such as some of the Freons.

Data gathering can begin when the test chamber and support equipment, the drop forming mechanism, and the photographic and timing apparatus are available. A block diagram of the layout of this apparatus and its support equipment is included as Fig. 2. This much of the apparatus is capable of

yielding drop position vs. time and drop diameter vs. time for given initial

drop diameter and chamber temperature and pressure. While such data is being

taken, the design, construction, and testing of devices with which to measure

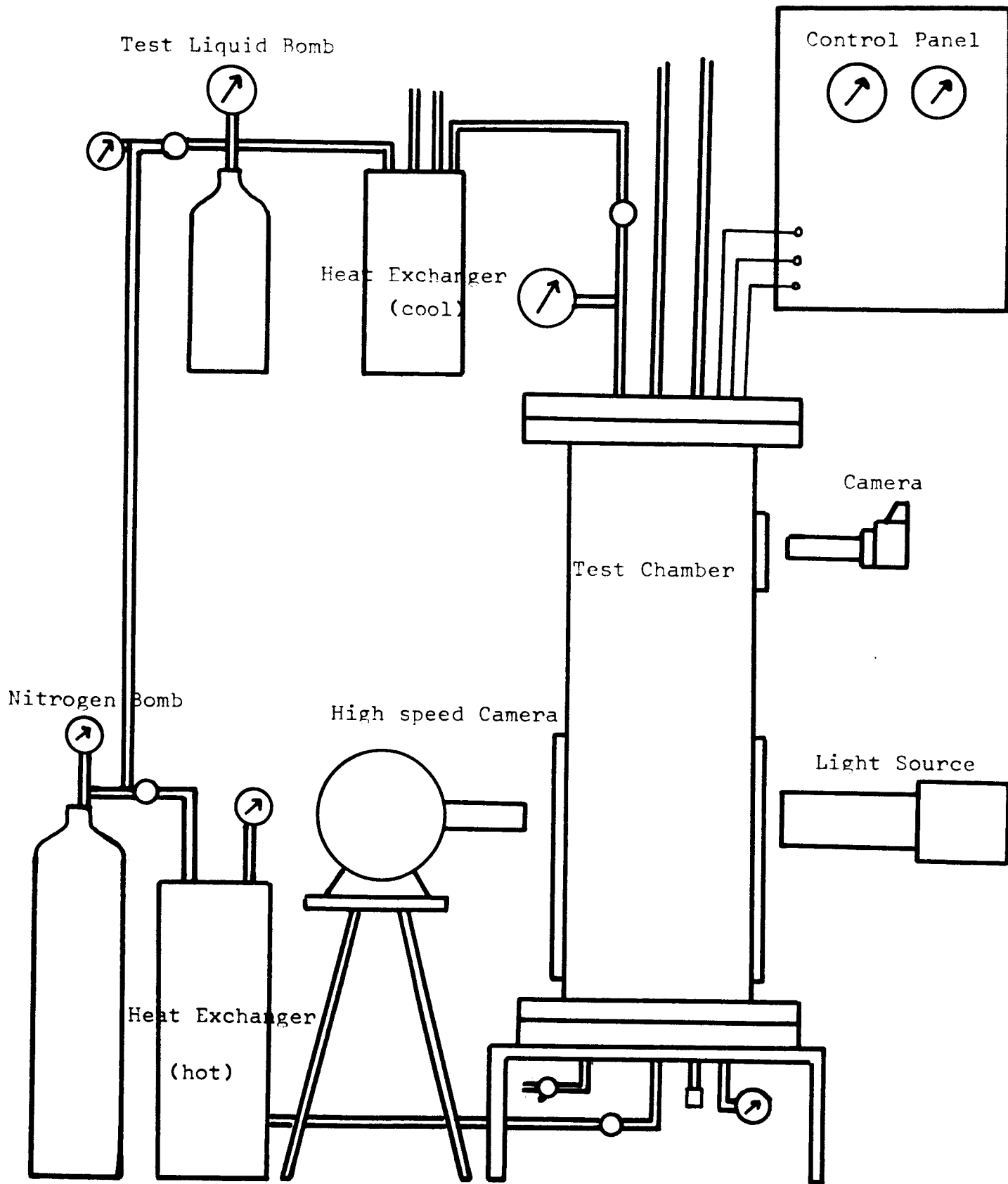droplet temperature and droplet mass will be carried forward.

Fig. 2

Schematic of the Falling Drop Experimental Apparatus

IV. HEAT TRANSFER WITH PULSATING PRESSURES

A. WITHOUT MASS FLOW

The purpose of this project is to study the heat transfer behavior of a gas under the influence of periodic pressure and temperature fluctuations in a closed system. The system used to produce periodic fluctuations is air in the cylindrical combustion chamber of a small, high-speed, motored internal-combustion engine. The principal variables measured are gas pressure, gas temperature, wall surface temperature, and driving frequency.

Gas temperature is followed by measuring the resistance changes of a fine resistance wire. In order to protect this wire from impact with oil droplets, a nonlubricated piston-cylinder system, using teflon piston rings, was obtained. Two teflon piston rings about 1/8 inch wide were placed on 0-rings in special ring grooves centered on the original ring grooves. Because of piston rocking and lack of cylinder lubrication, a great deal of scuffing on the piston skirt and cylinder liner were noted; after 45 minutes of running, the piston and cylinder liner needed replacement. The replacement piston was fitted with a very thin teflon ring at the base of the skirt to provide support against side thrust. This piston-cylinder has run for approximately 2 hours at about 600 rpm with very little scuffing.

Piston ring wear was at one time considered to be a limiting factor. Ring wear has been measured and amounted to a maximum of only .0045 inch in rings .0750 inch thick after two hours of service. Total ring wear, four

or five times this amount, can be tolerated before the rings will need replacement.

A multiple cam-breaker point assembly driven at engine frequency off the crankshaft was designed and constructed as the major part of the calibration circuitry for the resistance wire and the surface thermocouple. A system, triggered by the engine breaker point, was built to provide the Tektronix oscilloscope with a 10-volt square wave for synchronization. A set of five ground locating surfaces was designed and installed to facilitate realignment of the engine and the cam-breaker point assembly after removing them for machining or parts replacement.

A drum camera, supplied by the Department of Mechanical Engineering, was found to take acceptable film records of the oscilloscope traces inside or outside of the remote darkroom, so the equipment was removed from the latter and reassembled near the engine. The drum camera controls were modified slightly to suit test purposes. Data are recorded on a film with an exposed area of 1.9 inches by 29.4 inches. Optimum exposure and developing parameters were determined by trial and error. On most runs, the temperature and pressure signal amplitudes on the film are on the order of 1.1 inches. This corresponds to about 1.7 inches on the oscilloscope face. The line width on the film is on the order of .015 inch. One cycle is typically 14 or 15 inches in length, so that a one crank-angle interval extends greater than 1/32 inch on the film.

Low-noise Astrodata amplifiers are used as high-gain preamplifiers, and a Tektronix 4-beam oscilloscope is used at low gain for signal display.

The Astrodata preamplifiers are low noise, linear-phase, differential input amplifiers; as they introduce a frequency-dependent phase shift into the signal, all signals displayed on the oscilloscope pass through these pre-amplifiers so that they undergo a uniform phase shift. Preamplifier gain for the surface thermocouple is 3000; for the resistance wire bridge signal, 500; for the pressure pickup charge amplifier signal, 12; and for the timing mark pickup, 10.

The mounting of the fine resistance wires constituted a problem of no small magnitude which was solved in the six-month period. The active length of the Platinum-10% Phodium wire is bonded to two constantan support wires with insulating epoxy cement. The electrical signal is carried out through two UNC 2-56 machine screws, insulated with miniature fiber washers and electrical spaghetti, to which the wire is soldered. A wire of this type, of .00012 inch (3 micron) diameter and 3/8 inch length, has lasted for 48 minutes at speeds up to 1200 rpm without failure. The nominal dc resistance of this wire is 150 ohms, and the estimated phase lag of this wire, due to its finite size, is about 1.5 crank angle degrees at 1200 rpm.

Some time after these resistance wires were constructed and run, communication with Zitzewitz Engineering Associates, a New Jersey manufacturer of hot wire anemometers, revealed that they now have the capability to make anemometer probe wires one millimeter long and less than one micron (.00004 inch) in diameter in their laboratory. These wires are solid tungsten, microwelded to gold-plated nickel supports. The use of tungsten, microweld

supporting, and very short lengths will increase the wire strength by a factor of at least ten (as compared to a conventional wire of the same diameter), permitting the use of wire diameters less than one micron, with consequent great increase in wire response. A one-micron tungsten wire has an estimated thermal lag of less than one crank angle at 4000 rpm. Four of these probes have been on order for over a month. The nominal resistance of these probes is on the order of six ohms, so the design and construction of a satisfactory bridge is not as easy as for a wire resistance of 150 ohms, because of the effects of cable, connector, and lead resistances. Two channels of bridge and calibration circuitry have been built, as have instrument plugs and probe supports, and await the arrival of the probes.

An even better probe for this type of measurement would have a small, strong, insulating fiber with a very thin conductive coating replacing the solid resistance wire, since the instrument would have high resistance (a film of .05 micron platinum (.00002 inch) on a 10 micron quartz fiber has 87 ohms/mm), great strength (10 micron fused quartz fibers have 130,000 psi tensile strength), and very fast response (less than 0.1 crank angle at 6000 rpm). Thermo Systems, Inc., of Minneapolis, manufactures a probe made of 25.4 micron diameter glass rod coated with an active length of .010 in. of platinum, mounted on gold-plated stainless steel supports. Communication is presently going on as to whether the glass rod diameter can be reduced to 10 microns or less (since a larger sensor probably expert a disturbing influence on its environment) and the active length increased by a factor of three or four.

During th. past six months, seventeen low-speed data runs with film records were taken with the object of establishing data taking procedures, check out the calibration mechanisms, examine the requirement of equilibrium, and take some preliminary data. The results of one of these data runs are presented in Figures 3 and 4. Some of the data for Fig. 4 are:

pressure swing	= 341 psi
pressure peak	= 349 psia at -5.3 crank angle degrees
gas temperature swing	= 635 °F
gas temperature peak	= 7/3 °F at -8.2 crank angle degrees
wall temperature swing	= 4.3 °F
wall temperature peak	= 139.9 °F at +60 crank angle degrees
engine frequency	= 450 rev/min

If the analytical model is taken to be a cylinder of gas at a position-independent (but time-dependent) pressure and temperature surrounded by a thin boundary layer in which all temperature gradients are confined, and if we assume that the gas temperature measured by the wire is the temperature of this "bulk gas," then the mass of gas in the cylinder can be computed easily from the perfect gas law. When this was done for the data of Fig. 4, it seemed that the gas mass remained constant in the interval from 175 to 35 crank angle degrees before pressure peaked; the computed mass then decreased for 120 crank angles, during which time the pressure difference across the teflon rings was high. When makeup air ports were exposed by the piston, the computed mass showed an increase to the initial value. This suggested a relatively large leakage past the teflon rings. Further analysis of the data cast doubt as to whether a real mass loss took place. More data will be taken and analyzed in an attempt to determine the reasons for the computed change in mass. A constant

GAS PRESSURE (100 PSI
SQUARE WAVE SUPERIMPOSED)

WALL TEMP

GAS TEMP

-180

-90

-70

TDC

+90

TIME ⟶
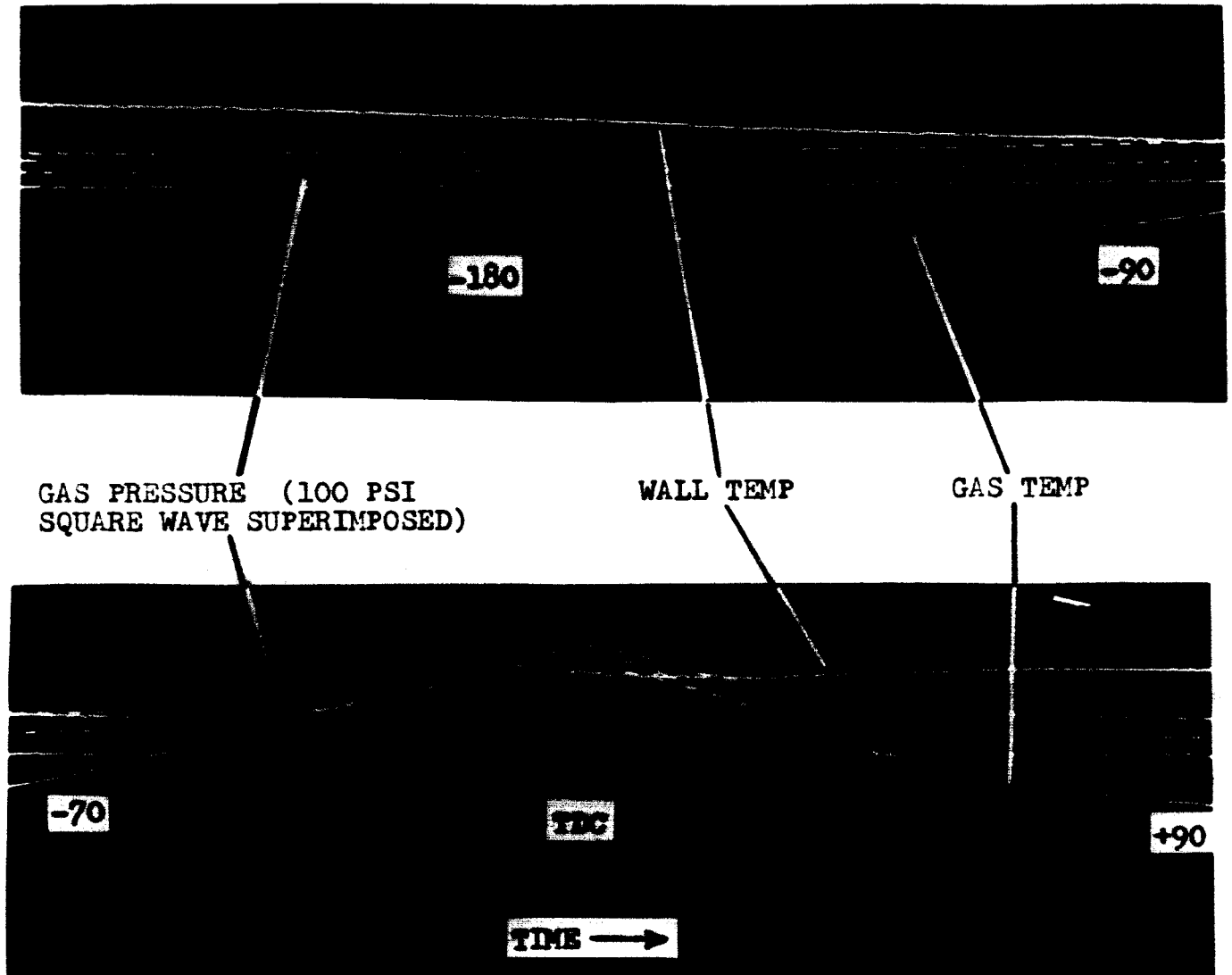
ENGINE SPEED 660 RPM (11 CPS)
WALL TEMP SWING   6.3 F°
GAS TEMP SWING   559 F°
PRESSURE SWING   390 PSI
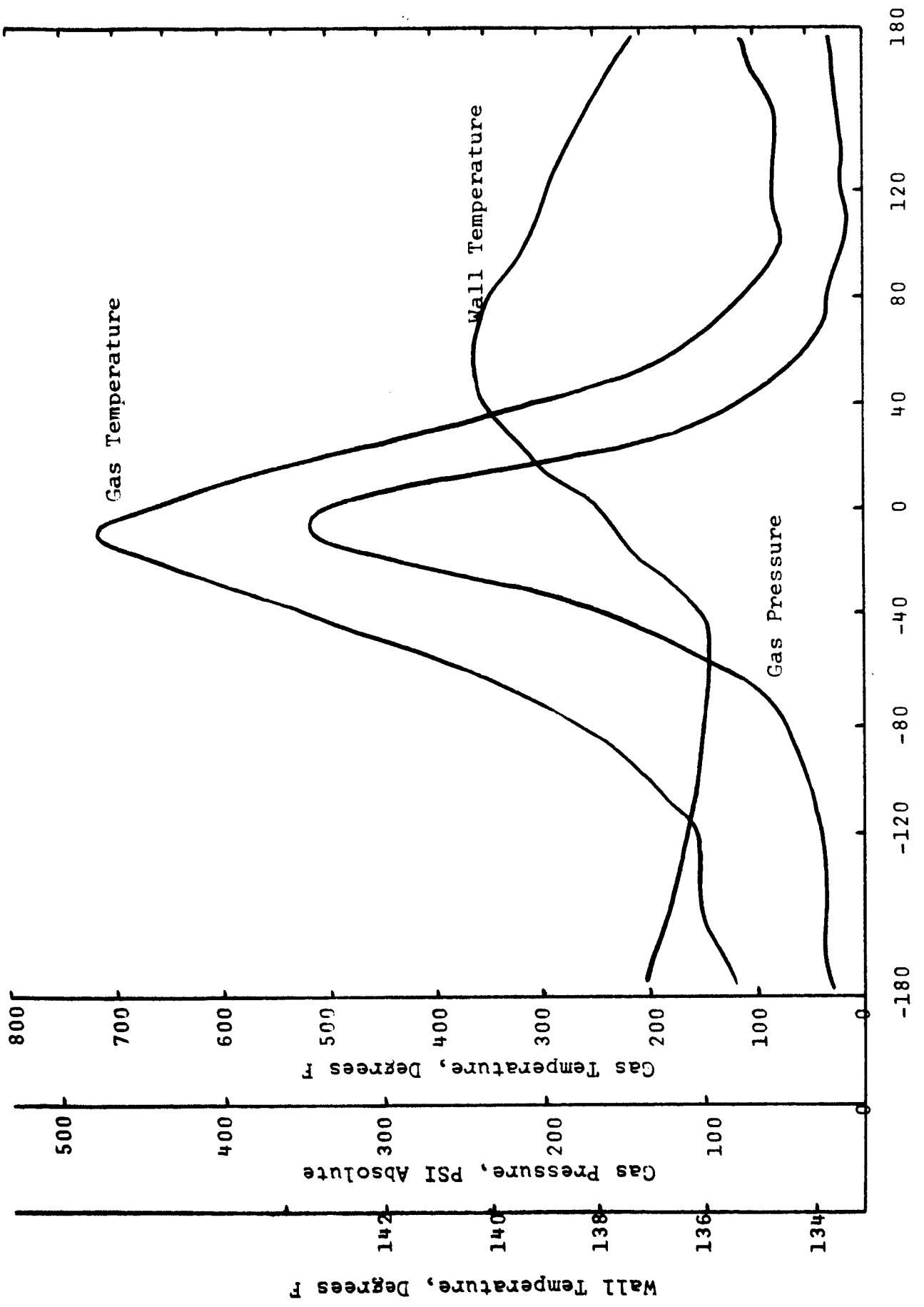
FIGURE   3   A PORTION OF A TYPICAL CYCLE OF DATA

Gas Temperature

Wall Temperature

Gas Pressure

Crankangle Degrees

Figure 4

Gas Temperature, Degrees F

Gas Pressure, PSI Absolute

Wall Temperature, Degrees F

mass is to be desired if correlation of experimental results to analytical models is to be attempted.

Some effort was expended in the direction of an analytical treatment of the problem. The analytical model is one-dimensional, with the system being the time varying gas volume contained between head and piston, plus the mass of the head. The piston surface and head exterior temperatures are taken as constants. This analysis awaits an experimental determination of how constant the mass is with time.

Programs for the Fourier analysis and term-by-term heat transfer treatment of the wall surface temperature (the object of which is instantaneous wall heat transfer) are in a shakedown status.

The primary effort in the next six month period will be to obtain and analyze data. The head and cylinder will be preheated to different temperatures to ascertain if this will help the system reach equilibrium faster. The engine speed will be varied as a primary independent variable.

When the solid tungsten wire anemometer probes arrive, they will be installed to replace the longer Platinum-10% Rhodium wires and their performance will be evaluated. It will probably take three weeks after receipt of the probes to bring them to an operational status and take initial data as to their response; the probe diameter is only .112 inch, and they must be secured and operated in a very confined space. If the anemometer probes perform as expected, they should be durable and have relatively fast response.

Communication will continue with Thermo Systems, Inc., as to the manufacture and modification of platinum plated quartz fiber probes. If these probes can be obtained during the next six month period, they will be installed and evaluated. The expectation is that these instruments should have greater strength and less thermal inertia than any wire probes. A judgment will be made as to which of the resistance thermometer systems (suspended Pt-10% Rh wire, Tungsten anemometer probe, quartz fiber probe) is most suitable from the viewpoints of durability and thermometer response time, and the best one will be used for high-speed data runs.

Further data will be taken and treated to determine the nature of the leakage problem, if it exists. If a significant amount of leakage is noted, there are a number of corrective measures which can be taken. The compression ratio is being reduced from 11.9 to about 9 or 10 to reduce torsional oscillations in the crankshaft; this will reduce the pressure ratio from 32 to about 25. The crankcase can be pressurized somewhat to reduce the pressure differential across the teflon piston rings. As a drastic step, the piston can be redesigned to broaden the piston rings.

Some difficulty was experienced with the timing mark wheel shaking loose at speeds in excess of 1000 rpm due to the torsional oscillations in the crankshaft. The timing mark wheel has been machined to reduce its moment of inertia and a wider key with locking set screws is being fitted. It is hoped that these changes, coupled with a reduced pressure ratio, will be adequate to insure safe high-speed operation.

During pauses in the experimental efforts, work will continue on the techniques of heat transfer analysis of the data, on the treatment of the analytical model of the thermodynamic problem and on a simulation computer program for the cylinder which would treat the cylinder gas a thermodynamic system.

IV. HEAT TRANSFER WITH PULSATING PRESSURES

B. WITH MASS FLOW

The purpose of this project is to study the heat transfer behavior of a flowing gas near its stagnation point on a wall normal to the flow direction when large amplitude, high frequency ($\approx$ 1000 cycles/sec) pressures waves are superimposed on the flow. The system consists of a long pipe with a siren at one end which introduces the pulsating flow and a flat plate test section normal to the pipe axis at the outlet end.

As a result of the noise which will be generated by this apparatus, it was necessary to find a suitable location for it. It was finally decided to convert a basement storage room into a research laboratory. This particular room was chosen because of its remote location and because the major portion of the walls is reinforced concrete, which minimizes the amount of sound-proofing needed. The research apparatus is to be located inside this room which will be referred to here as the test cell. An area adjacent to the test cell has been partitioned off in order to provide a control room for the apparatus.

To eliminate potential noise leaks from the test cell, all pipes which pass through the room have been covered with fine glass wool yarn. The door has been covered with a sheet of lead impregnated vinyl and sealed with felt weather stripping. No further soundproofing is planned until the apparatus becomes operational and the level of the noise generated is determined.

Because of the use previously made of this area, extensive electrical

work was necessary in converting it to a usable research space. This electrical work is currently in progress and should be finished in a matter of a few weeks. The high pressure air compressor, along with the air supply cylinders and the associated manifold, has been installed in the test cell. This compressor is one that was obtained as a surplus item from the Air Force and has been overhauled extensively since its acquisition.

The design of the apparatus has been underway for some time now. The resonant condition in the pipe is to be obtained by rotating the disk at a fixed speed and its timing is accomplished by varying the length of the pipe between the siren disk and the test section. The variation of the pipe length is accomplished by two means: (1) spacers with a length range of from one to six inches in one inch increments, and (2) a telescoping section which provides a continuous adjustment of up to 1.25 inches. Therefore, with the combination of the two, it is possible to provide for any adjustment up to 7.25 inches. In series with the telescoping section and the spacers is the main pipe, whose length is on the order of seven feet. Adjustments greater than 7.25 inches can be made by having several main pipes of different lengths.

The working drawings for the above-mentioned pipe adjustment assembly and the test section assembly are to be submitted to the shop for construction in the near future. In order to minimize air leakage from the siren, it is necessary to enclose the siren disk in a pressurized housing. For this purpose, an old steam turbine housing with a pressure rating of 450 psig has been obtained.

At present, the design of the siren is being delayed until the turbine housing arrives so that the nature of the necessary modifications can be determined.

It is expected that the design of the apparatus will be completed by the first of the year and that construction would start shortly thereafter. Barring unforseen difficulties during the construction and installation phase, preliminary shakedown of the apparatus should occur within the next six months. Within this same time period, a familiarity with the heat transfer problem will be obtained by treating a highly idealized model of the problem so that potential flow theory can be used. Although it is realized that the actual solution of the problem is a boundary layer one, nevertheless, it is felt that there are definite benefits to be obtained by considering the simplest possible model as a starting point for the theory.

V. DROP SIZE AND VELOCITY DISTRIBUTION MEASUREMENTS

A. VELOCITY DISTRIBUTION MEASUREMENTS

At the end of the previous reporting period, data had just been taken on the sizes and velocities of droplets in a spray using a double flash fluorescent photographic technique. In order to make use of this raw data, it must be processed manually. Each film is divided into 80 sections. Drop pairs in each section are identified as in good or bad focus and their diameter, speed, and angular direction of travel measured. Approximately 20% of the 444 films have been read at Wisconsin so far and the resulting data punched on cards. This represents about 10,000 data points. Similar data processing is also being done by John Groeneweg. Analysis of all of this data is currently being carried out by John Groeneweg (who is now at NASA -Lewis Laboratories) as part of his Ph.D. thesis.

Since the utility of the spray work can best be judged after the analysis of the data has been completed, and since there is a shortage of students to work on the various projects, it seemed wise to delay further work on sprays and to devote more effort to the vaporization work reported in part III C of this report.

It should be mentioned that Dr. Hiroyasu has been studying the use of different drop size distributions in representing experimental data. Since the material has not yet been edited, it is not included with this report but will be included with the next report.

V. DROP SIZE AND VELOCITY DISTRIBUTION MEASUREMENTS

B. LASER STUDIES

One of the problems encountered in obtaining velocity distributions in sprays was the lack of a very short duration high-intensity light source. A laser light source was thus rented from Lear Siegler to determine the feasibility of using the laser in conjunction with the fluorescent technique. A report covering these experiments was prepared and is attached to this progress report. It is planned that Groeneweg, Sowls, and Hiroyasu will revise this report for suggested publication as a NASA TN.

A TEST OF THE FEASIBILITY

OF USING A LASER AS A LIGHT SOURCE

FOR PHOTOGRAPHING SPRAYS

Report Prepared By

Hiroyuki Hiroyasu

Richard Sowls

August 1965

The experiment covered in this report
was suggested and organized by John Groeneweg,
now with NASA at the Lewis Research Center in
Cleveland, Ohio. The people that participated
in the experiment were John Groeneweg, Hank
Laughlin, and Ronald Barker with the Lear Sieg-
ler Laser Systems Center and H. Hiroyasu and R.
Sowls with the Engineering Experiment Station
of the University of Wisconsin.

INTRODUCTION

Photographing fast moving drops in a spray using the fluorescent technique requires a light source that gives a very short pulse of light of a suitable wavelength and of sufficient intensity to cause the drops to fluoresce strongly enough to be photographed. In addition, the nature of the light should not cause strange effects that make data reduction difficult or impossible.

To determine the maximum tolerable duration of the light pulse, suppose a drop that is moving at 100 m/sec is being photographed by a camera with a linear magnification of 25. The image on the film is moving at 2.5×10^6 mm/sec and the maximum tolerable motion blur on the film is 0.1 mm. Then the longest permissible light pulse, assuming that the decay time for the fluorescence is not significant, is $0.1/.25 \times 10^7$ or 40×10^{-9} sec or 40 nanosec. The constricted arc light source that is presently used with the fluorescent technique has a nominal duration at half peak intensity of 2 μsec or 2000 nanosec, i.e., at least 50 times longer than the desired value 40 nanosec. In contrast, the laser that is being investigated here gives pulses of about 20-50 nanosec.

Conservative calculations indicate that for the constricted arc light source the maximum amount of light energy per pulse arriving at the space being photographed is of the order of .0001-.0002 joule. For comparison, the laser that was investigated here is capable of outputs up to 1.0 joule per pulse of

ruby light (6943 Å), and the harmonic generator is capable of
providing 0.01-0.02 joule per pulse of ultra-violet light (3471 Å).

PURPOSE OF THE EXPERIMENT

The experiment was conducted to test the feasibility of
using a ruby laser with a KDP harmonic generator as a light
source for photographing sprays by the fluorescent technique.
It was suspected beforehand that the pulse duration (20-50
nanosec) and the .01-.02 joule per pulse output of ultra-violet
light would make this combination a very suitable light source
for use with the fluorescent technique. The questions to be
answered by the experiment were: 1) Will the single wavelength
available (3471 Å) cause the droplets to fluoresce strongly even
though it is very low on the absorption curve of the fluorescent
dye (see Fig. 2)? This is important because no dyes could be
found for which 3471 Å light is high on the absorption curve.
2) Does the special nature of laser light (monochromatic, plane
polarized, and coherent) cause any strange effects which make
it unsuitable as a light source; i.e., can the true drop size
be easily determined from the photographs? 3) Is the laser and
KDP cell combination that was used in this experiment a suit-
able light source for photographing sprays by the fluorescent
technique?

Aside from these main points, there are the possibilities
of using ruby light (6943 Å) either to photograph droplets by
scattered light using red sensitive film, or by the fluorescent

technique if a suitable fluorescent dye and infrared film combination could be found. Because no such dye and film combination was available, only the scattered light method was tested.

APPARATUS USED

Fig. 1 is a block diagram of the layout of the apparatus used in the experiment. A brief description of some major components and their functions follows.

Laser System

The laser used was a Lear Siegler Model LS-1400B. This is a Q-switched ruby laser which is capable of 0.3-1.0 joule single pulses of ruby light (6943 $\overset{\circ}{A}$), 20-50 nanosec long. Part of the ruby light is converted to ultra-violet by the KDP (potassium dihydrogen phosphate) cell which is also a Lear Siegler product. This cell can provide about 0.01-0.02 joule of ultra-violet light per pulse. The $CuSO_4$ filter is used to absorb the remaining ruby light while transmitting the ultra-violet.

Camera

The camera was specially constructed for photographing droplets using the fluorescent technique. It uses a two lens system to obtain a linear magnification of 25; it has a minimum f number of 5.6, and it uses 4 x 5 sheet film. Note from Fig. 1 that the camera axis, the spray axis, and the laser beam are mutually perpendicular.

SPARK LIGHT SOURCE

QUARTZ
LENSES

NOZZLE

CAMERA

SIMPLE
LENS

KDP   CuSO₄
CELL   FILTER

CONTROL AND
POWER UNIT

LASER HEAD

ENERGY
STORAGE UNIT
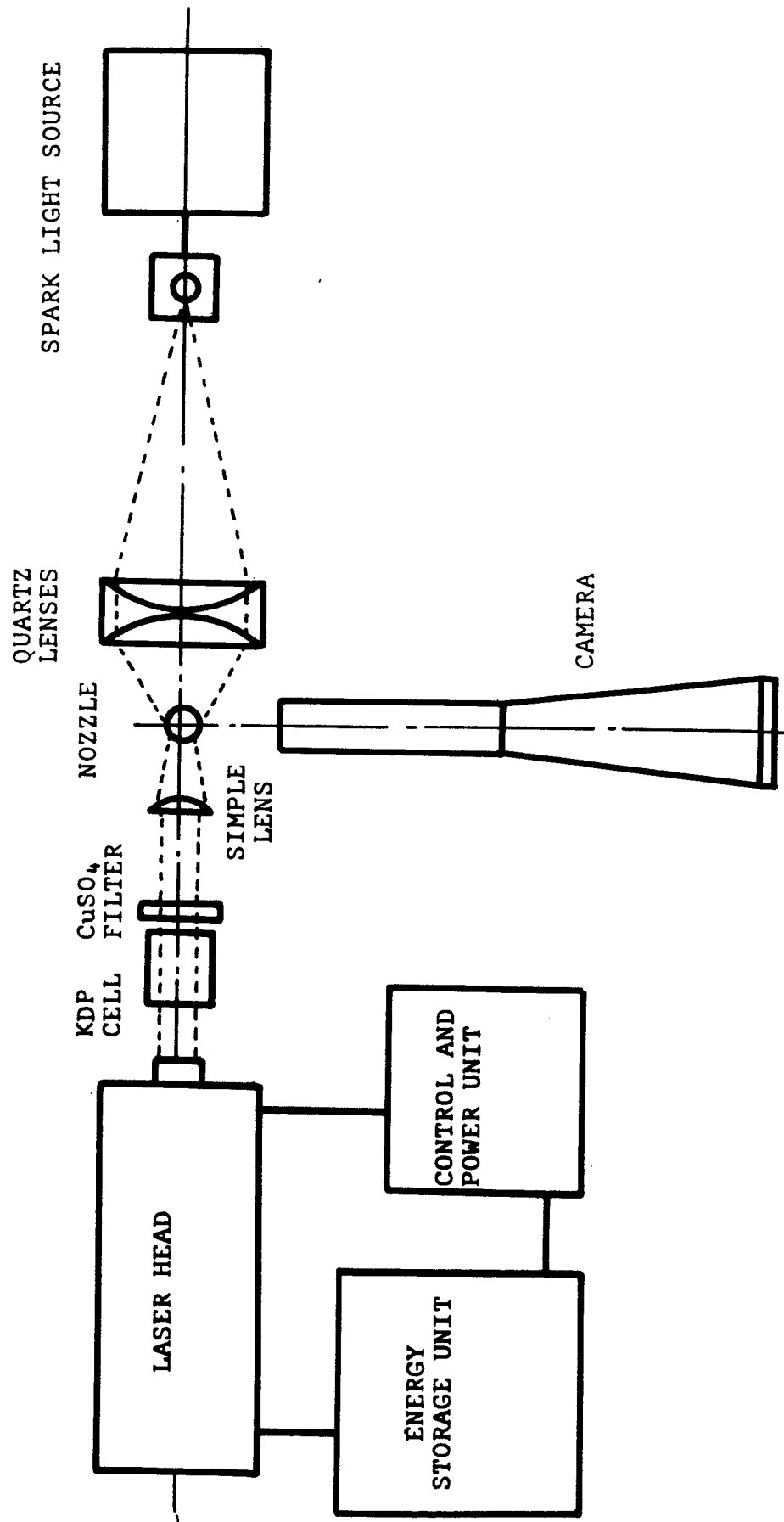
Fig. 1 – Block Diagram of Apparatus

Spark Gap Light Source

The most important details of the spark gap light source are that it discharges a 0.1 ufd capacitor previously charged to about 40 kv through a 1/32" wide, 1/2" high, 1/8" deep slot in a teflon block by means of a three electrode spark gap switch. The fused quartz condensing lenses form an image of this "line" light source in front of the camera. The illuminated space in front of the camera is about 4 x 5 x .2 mm.

Fluorescent Dyes

The spray liquid used in the experiment was 95% ethyl alcohol containing a fluorescent dye. Absorption-emission curves for the two dyes used (Fluorescein Uranin, and Rhodamine B Extra) are given in Fig. 2. These curves are not for the exact solutions that were used but should be similar to such curves. From these curves it can be seen that the 3471 $\overset{\text{o}}{\text{A}}$ light available from the ruby laser KDP cell combination is low on the absorption curves of both the dyes and the peak emission of Fluorescein Uranin is on the green end of the visible spectrum while the peak of the emission curve for Rhodamine B Extra is on the red end. The different peaks in the emission curves of different dyes may be useful in mixing studies.

The Fluorescein Uranin solution consisted of 5 gm/liter of the dye in 95% ethyl alcohol, while the Rhodamine B Extra solution contained 4.5 gm/liter of the dye in 95% ethyl alcohol.

absorption spectrum
.... fluorescence band

URANIN

ruby wavelength

RHODAMINE B EXTRA

ruby wavelength

INTENSITY, I

WAVE LENGTH, Å

WAVE LENGTH, Å
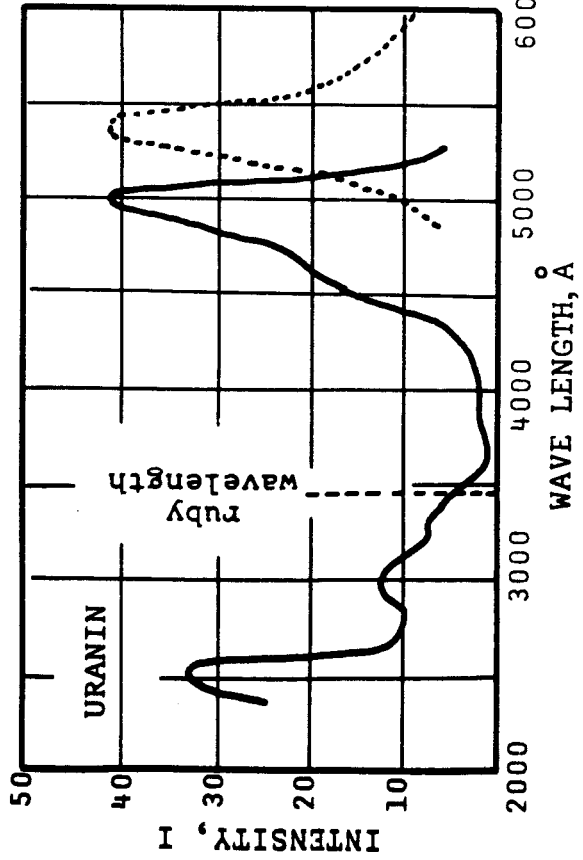
(a) Uranin
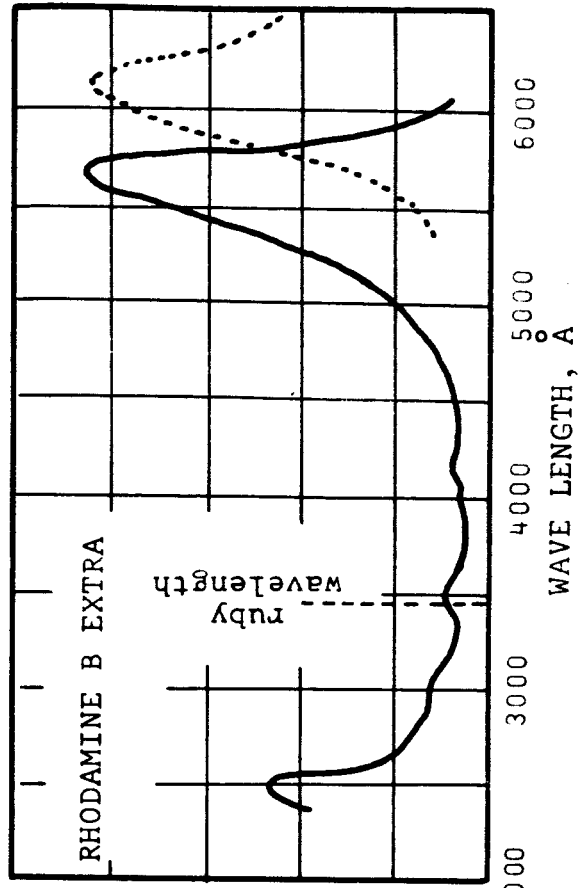
(b) Rhodamine B Extra

Fig. 2 – Absorption-Emission Spectrum in Ethanol

Films and Developers

Table 1 shows the films, developers, and developing times that were used in the experiments.

DATA AND DISCUSSION

In this experiment, photographs were taken both of single drops suspended from a 0.7 mm diameter hypodermic needle and of drops sprayed from a Monarch F-80 swirl type nozzle.

Single Drop Photographs Using 3471 $\overset{\circ}{A}$ Light

Photographs of single drops of pure ethyl alcohol, milk, ethyl alcohol containing Fluorescein Uranin, and ethyl alcohol containing Rhodamine B Extra were attempted using 3471 $\overset{\circ}{A}$ light. The pure ethyl alcohol drop did not expose Polaroid 3000 ASA film at all. The milk drop exposed the film slightly but showed no unusual effects, possibly due to the very weak exposure, too weak to be reproduced and included here.

Examples of the photographs taken of single drops of Fluorescein Uranin in ethyl alcohol and Rhodamine B Extra in ethyl alcohol are shown in Fig. 3a and 3b respectively. Fig. 3 is presented to compare the images produced by the two dyes on the same film (Royal X Pan). Note that both photos show ring patterns but that the rings in the Rhodamine B Extra drop appear slightly smaller. To the eye, Uranin and Rhodamine B Extra appear to fluoresce with equal brightness when they are illuminated by 3471 $\overset{\circ}{A}$ light. Probably the difference in the image density
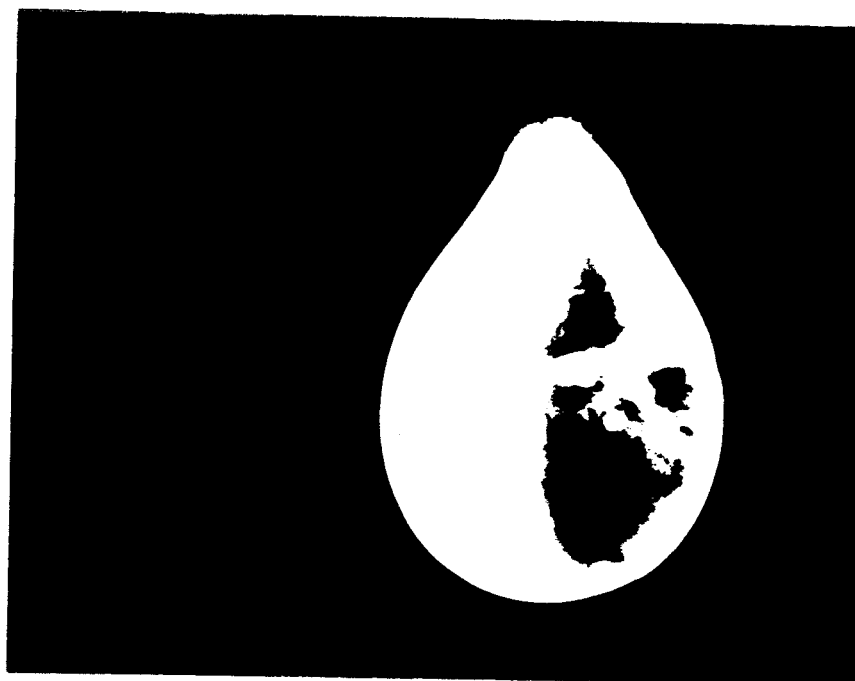
(a) Uranin
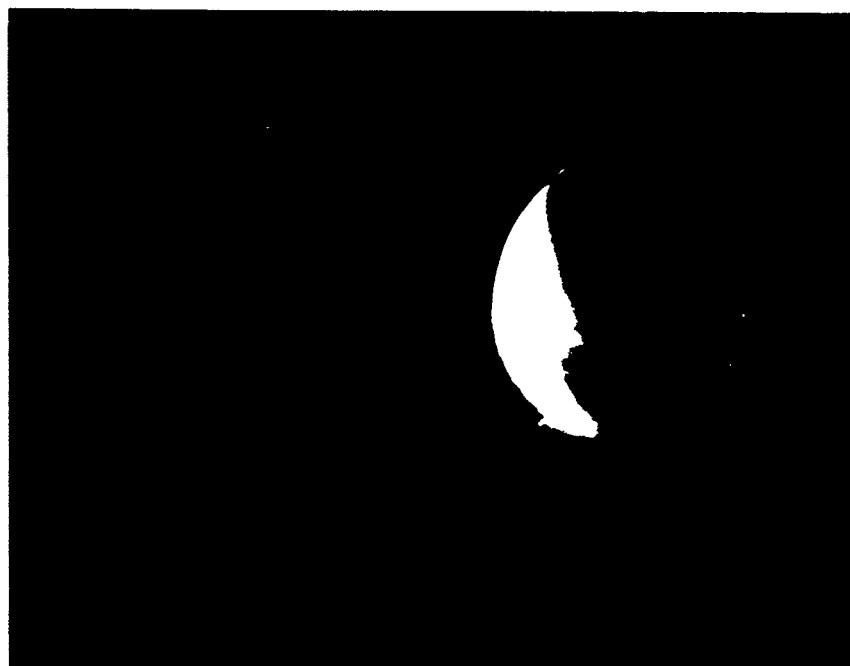
(b) Rhodamine B Extra

Fig. — Single Drops Photographed by Laser Light.

TABLE I

Films, Developers, and Developing Times at 68°F.

NAME	ASA No.	MANUFACTURER	SENSITIVE RANGE	DEVELOPER	TIME
Super Hypan	500	Ansco		D-11	5 min
Royal X Pan	1250	Kodak	360 $\overset{\circ}{A}$ ~ 350 $\overset{\circ}{A}$	DK-60a	12
Super XX	200	Kodak		DK-60a	9
2475	1600	Kodak	~ 720 $\overset{\circ}{A}$	DK-60a	6
Polaroid-57	3000	Polaroid			

between the two pictures is primarily caused by the spectral sensitivity of the film.

Fig. 4 illustrates the various patterns that were observed in single drops of the ethyl alcohol-Uranin solution that were suspended from a hypodermic needle. Fig. 4a shows two hot spots, 4b and 4c show ring patterns, and 4d shows a parallel strip pattern that appeared in several photographs. More evidence is needed before the cuases of these patterns can be specified but the following ideas are offered. The two hot spots in Fig. 4a may occur where the incident ultra-violet light is brought to a focus inside the drop by the shape of the drop itself. The rings appearing in Figs. 4b and 4c may be Airy rings that occur when a small region of a drop fluoresces with only a single wavelength or a narrow band of wavelengths during the time that the film is being exposed. The fact that the rings are nearly the same size for Uranin (which fluoresces green) and for Rhodamine B Extra (which fluoresces red) seems to contradict the idea that these are Airy rings unless they are due directly to the incident light from the laser system ($3471 \overset{o}{A}$, $6943 \overset{o}{A}$). Also, increasing the f number of the camera lens seems to decrease the size of the rings which is opposite to the usual behavior of Airy rings. A photograph was taken of a single drop of carefully filtered solution to see if the rings originate at suspended dye particles. This photograph was in no way different from a photograph of a drop of the unfiltered liquid. The parallel strip pattern shown in Fig. 4d seems to be the result of a stress pattern of some kind in the drop.

(a)

(b)

(c)

(d)
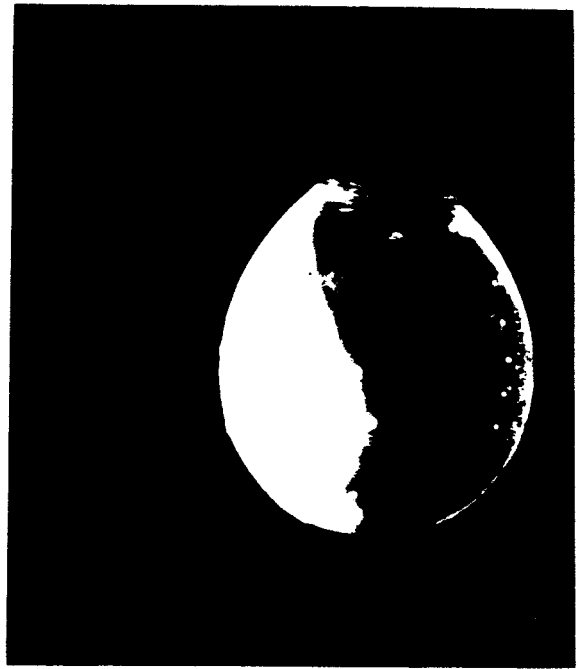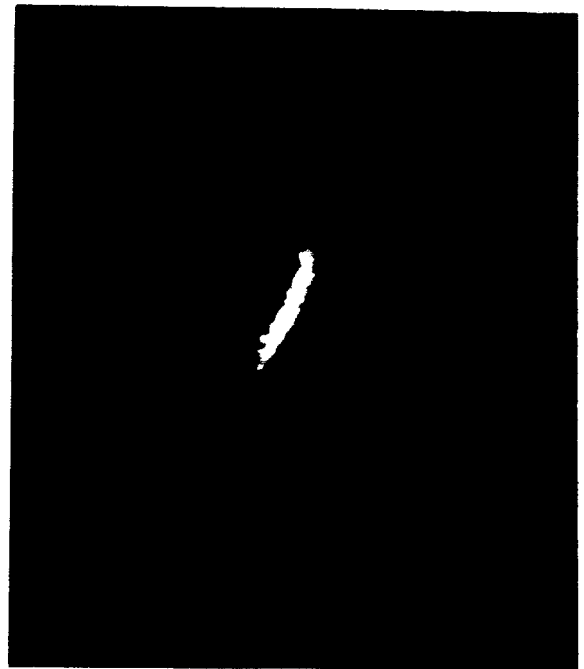
Fig. 8 - Drop Photographs Showing Patterns.

Fig. 5 gives two examples showing material disturbance by incident light. The question raised by such photographs is how was the image of this material formed? Possible answers are: 1) the material was already there when the light pulse occurred, 2) the fluorescent dye was so highly excited that it took much longer than normal for the fluorescence to decay, and 3) the material actually moved that distance during the time in which the light pulse occurred. John F. Ready in an article titled 'Effects of Laser Radiation' in the Aug 65 Industrial Research mentions that plumes of material leaving the surface of metals struck by the beams of Q-switched lasers may have velocities as high as 2×10^6 cm/sec. This is of the same order of magnitude as the velocity of the material shown leaving the drop in Fig. 5a, assuming a 20 nanosec light pulse duration and no fluorescent afterglow. This suggests that a combination of (2) and (3) above may be correct with (3) being the major contributor. Fig. 5a was made by focusing the 3471 Å laser system light on the drop with a small lens while Fig. 5b was made with both 3471 Å and 6943 Å light by removing the $CuSO_4$ filter. The image in Fig. 5b was probably produced largely by scattered ruby light.

Spray Photographs Using 3471 Å Light

A region of a spray of Uranin-alcohol solution was photographed using 3471 Å light for several different conditions. The pressure drop across the nozzle was varied from 20 psi to about 300 psi with none of the corresponding photographs showing any motion blur. Different films were tried in order to observe

(a)

(b)
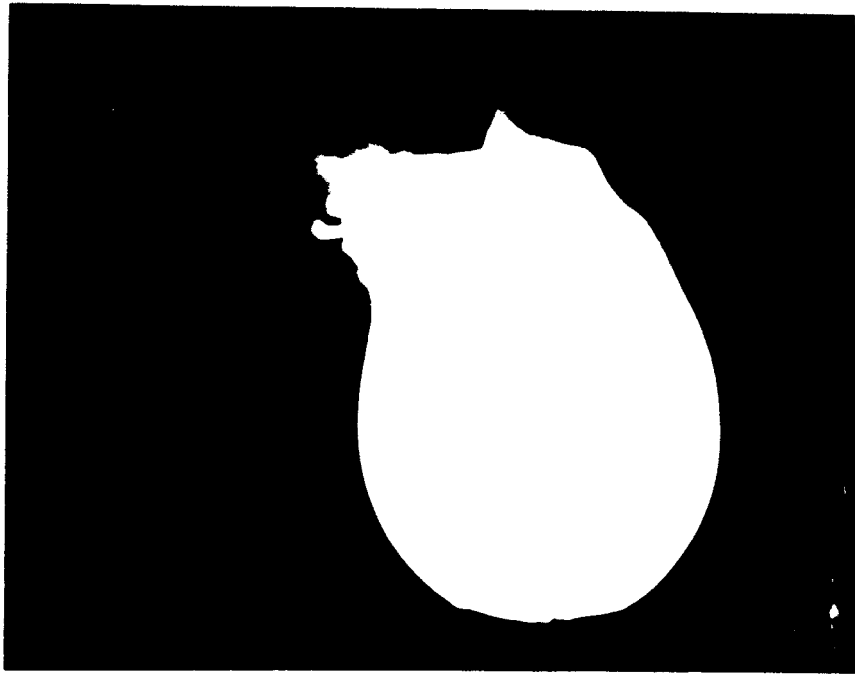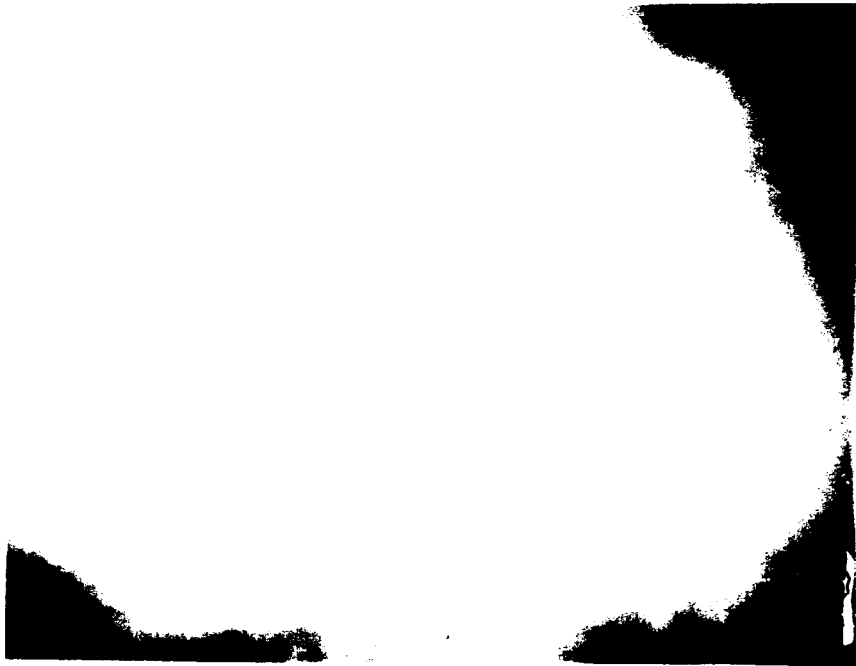
Fig. - - Photographs Showing Material Disturbance Caused by
Incident Light.

the effects of different degrees of exposure. The intensity

of the 3471 $\overset{o}{A}$ light incident on the spray was also varied.

Fig. 6 shows examples of spray photographs taken on

different films. Some of the important details that were

brought out by using films of different speeds have been lost

in these reproductions, but are given later in Figs. 8a, 8b,

and 8c. These pictures show that if cylindrical lenses can be

used to form a light sheet from the laser beam without destroying

much of the available light, a higher resolution but slower

speed film can be used than the Royal X Pan now used with the

constricted arc light source. They also show that it will not

be necessary to intensify the films as must now be done to obtain

sufficiently dense images.

Fig. 7a was taken with the 3471 $\overset{o}{A}$ light beam just as it

emerged from the copper sulfate filter while Fig. 7b was taken

using a small lens to concentrate this beam on the spray. Both

photos were taken on Royal X Pan. The intensity of the incident

light used to take Fig. 7b should be about 35 to 50 times the

intensity of the incident light used to take Fig. 7a. Much of

the difference in image density that distinguished the negative

of Fig. 7a from that of Fig. 7b has been lost in reproduction.

Still, it can be seen that the edges of the images in Fig. 7b

are much sharper than those in Fig. 7a. They are also very much

sharper than any images that have been produced under similar

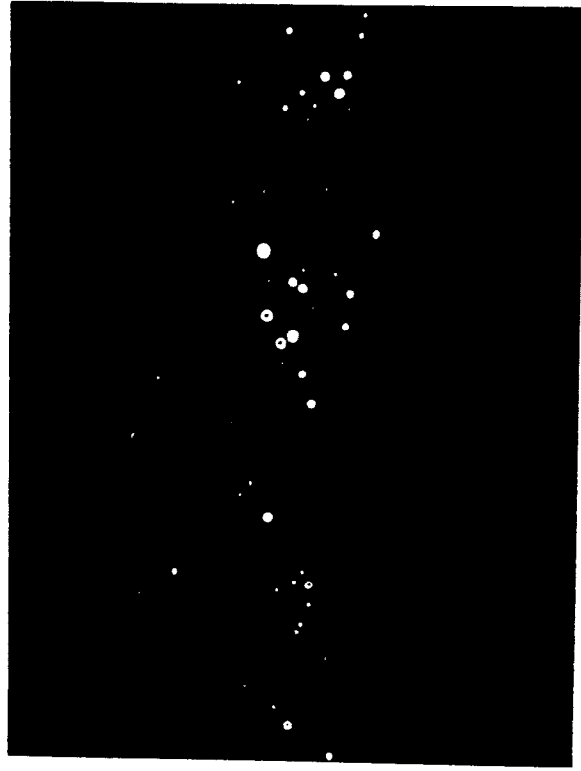conditions using the constricted arc light source. It can be

(a) Panatomic-X

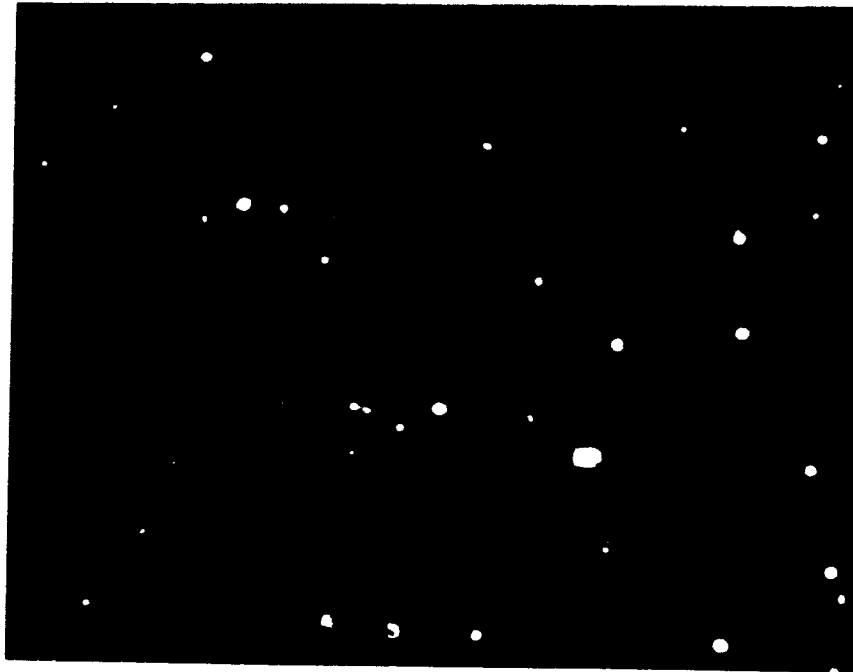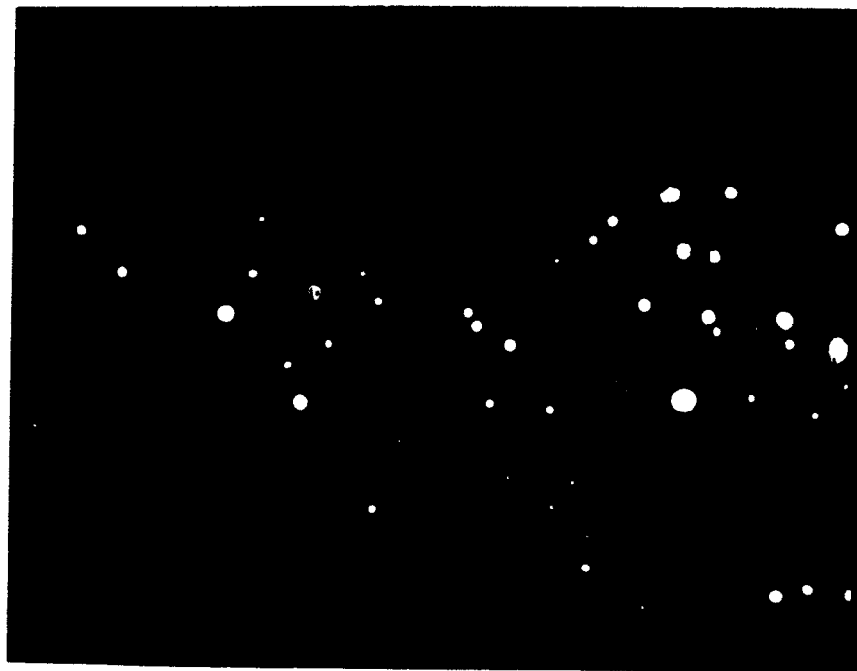(b) SXR-film pack

(c) XR-5 film

(e) Royal-X Pan
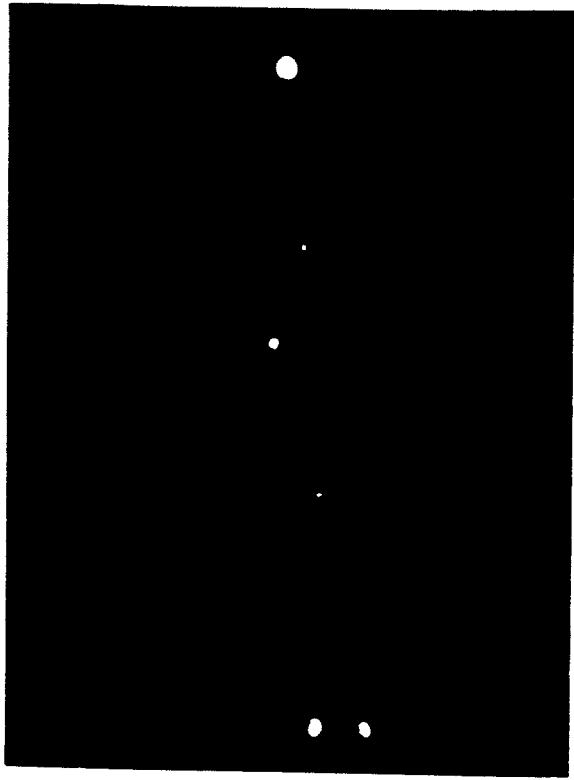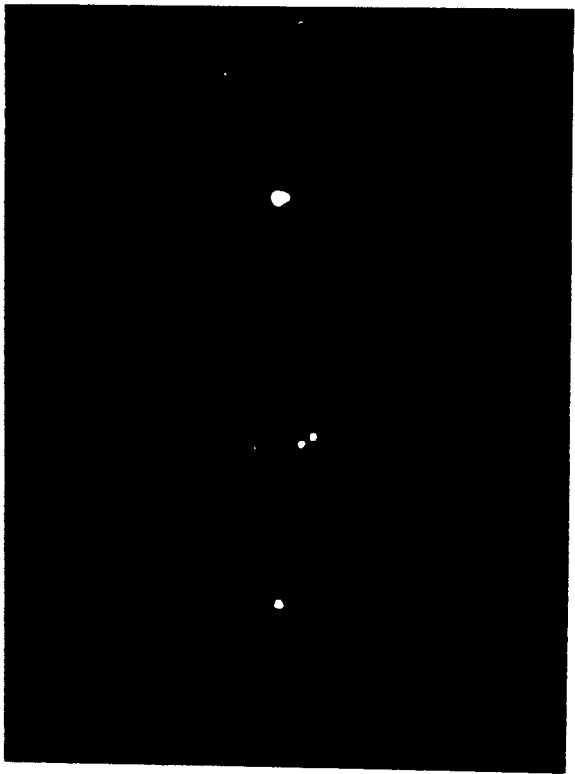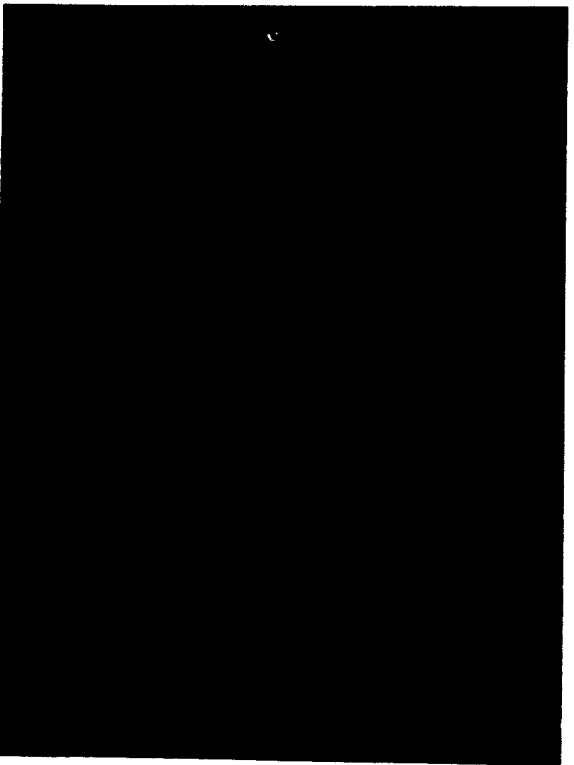
Fig. 6 - Spray Photographs on Different Films.

(a) Low intensity incident light

(b) Higher intensity incident light

Fig. 7 - Spray Photographs Showing the Effect of Incident
Light Intensity.

concluded from Fig. 7 that the light sheet must be formed as much as possible by focusing and not by just blocking out the unwanted light.

A photograph was also taken on Polaroid 3000 ASA film of a spray of Rhodamine B Extra in ethyl alcohol. This film showed that Rhodamine B Extra can be used with a suitable red sensitive film to produce sharp images of droplets in a spray.

Figs. 8a, 8b, and 8c are 15X enlargements from the negatives of the images of single drops from spray pictures taken using focused 3471 $\overset{o}{A}$ light. Figs. 8a and 8b were taken on Super Hypan film, and Fig. 8c was taken on Royal X Pan film. The images of drops that are strongly burned in are in good focus and appear as in Fig. 8c, perhaps a little irregularly snaped but with sharp edges. Images of drops which were in good focus but did not expose the film strongly enough to burn out the details nearly all exhibit some pattern or structure such as that shown in Figs. 8a and 8b. To determine if scattered 3471 $\overset{o}{A}$ or 6943 $\overset{o}{A}$ was causing any of these effects (including the ring effect that is not shown here), two green pass filters, a Corning 3385 and a Kodak #74 were tried on the camera lens. The resulting pictures differed from those taken without the filters only in that the image density was lower. From this it is concluded that these effects are not caused directly by scattered 3471 $\overset{o}{A}$ or 6943 $\overset{o}{A}$ light.
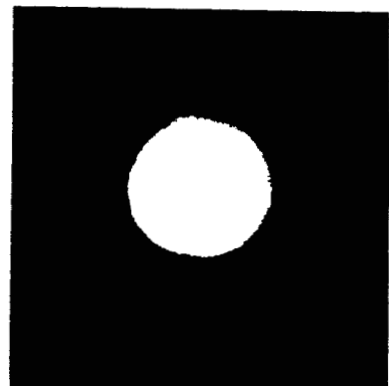
Fig. 8d is a 4X enlargement from negative size of a photograph taken of a spray using only 6943 $\overset{o}{A}$ light. Kodak 2475
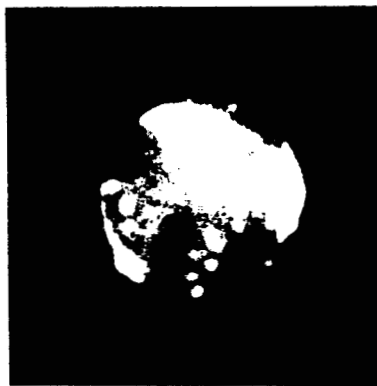
Fig. 4 - (a) Cell Structure Pattern, (b) Hot Spot Pattern, (c) Lumpy Pattern, and (d) Interference Patterns formed by Ruby Light Scattered from a Spray.

film was used. Due to the wide range of densities appearing

on the negative, much of the detail has been lost in reproduction.

The whole negative is covered with what appears to be overlapping

circular and straight interference fringes. It thus appears

that there is little hope for photographing drops by scattered

ruby light.

Spray Photographs Using Both 3471 $\overset{o}{A}$ Light and a Constricted Arc

Fig. 9 was included to illustrate how the apparent size of

a drop image taken using the 3471 $\overset{o}{A}$ light available from the

laser KDP cell combination compares with the size of the image

of the same drop using the constricted arc light source. The

photographs were taken by firing the laser first and then

firing the constricted arc light source about 10 μsec later.

Although some pairs of images of the same drop can be found,

so much detail was lost in reproduction that Fig. 9 does not

show much. Figs. 9a and 9b were taken with the intensity of the

light (3471 $\overset{o}{A}$) reduced to more nearly match that of the con-

stricted arc light source, while Figs. 9c and 9d were taken

with maximum intensity of the 3471 $\overset{o}{A}$ light.

Fig. 10 is a plot of drop size measured from the image

produced by the constricted arc light source against the size

of the image of the same drop measured from the image produced

by the laser KDP cell light source. About 80 drops were mea-

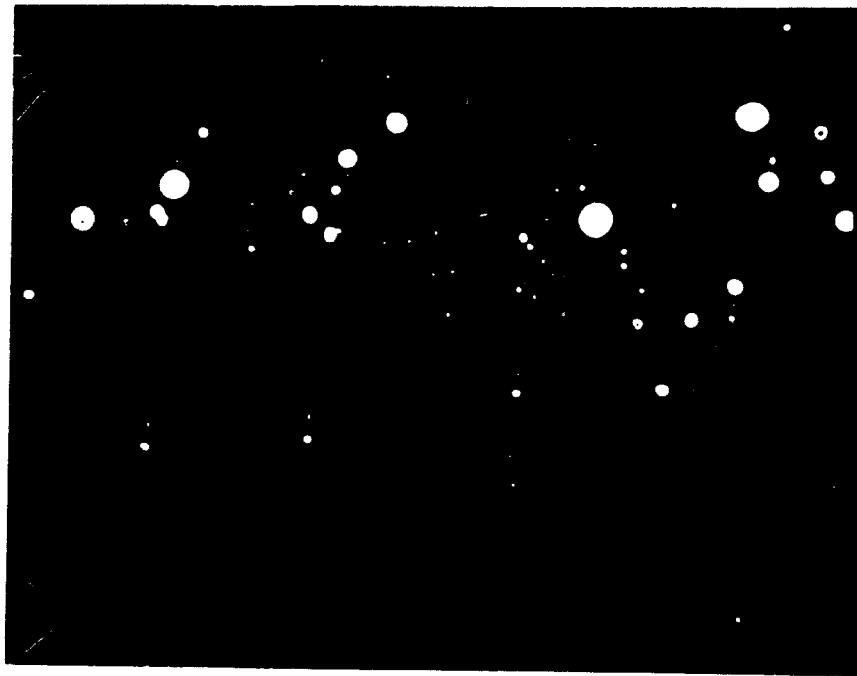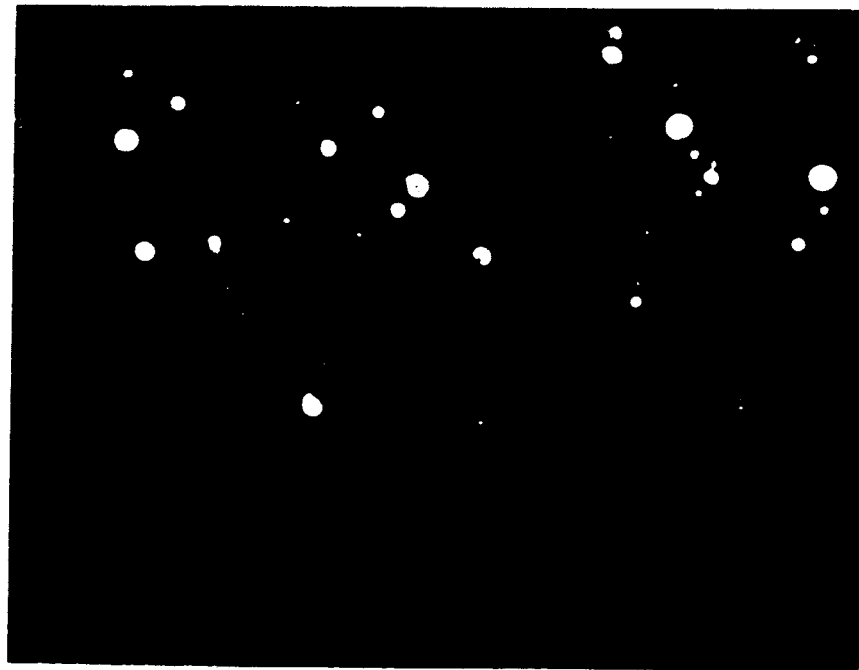sured from 20 films and are represented by the points on Fig. 10.

(a)

(b)
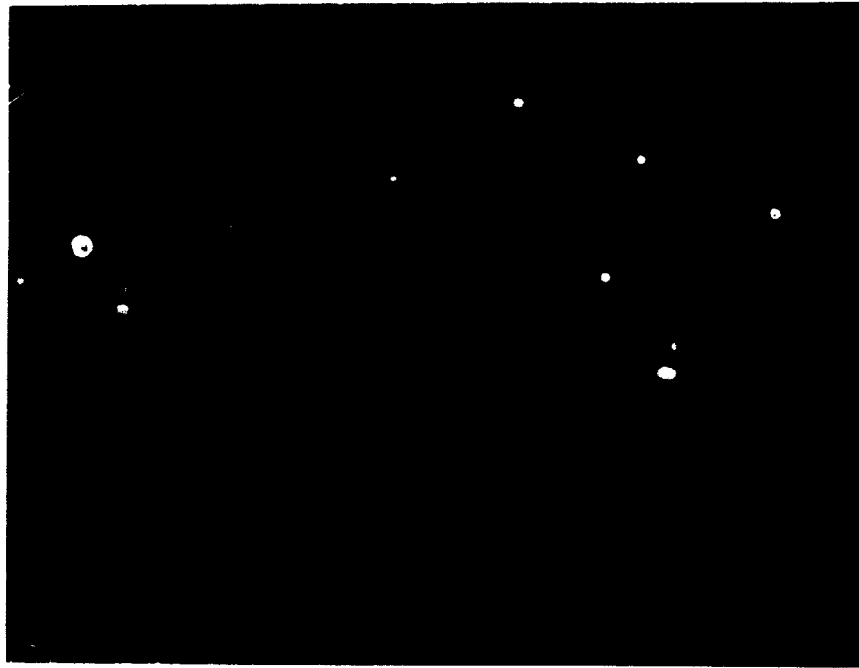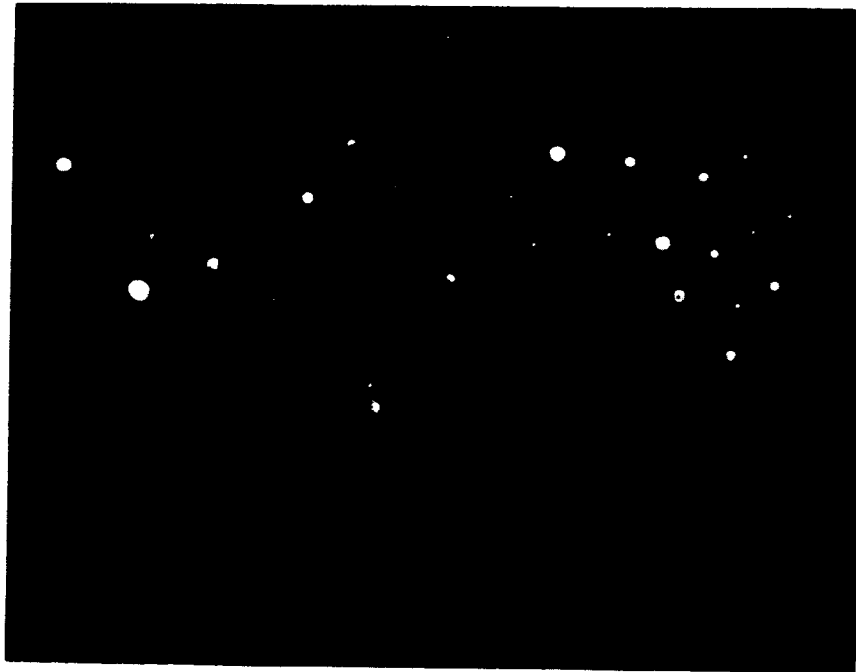
Fig. 7 - Double-Flash Photographs for Size Comparison.

(c)

(d)

Fig. 7 - Continued - Double-Flash Photographs for Size Comparison.
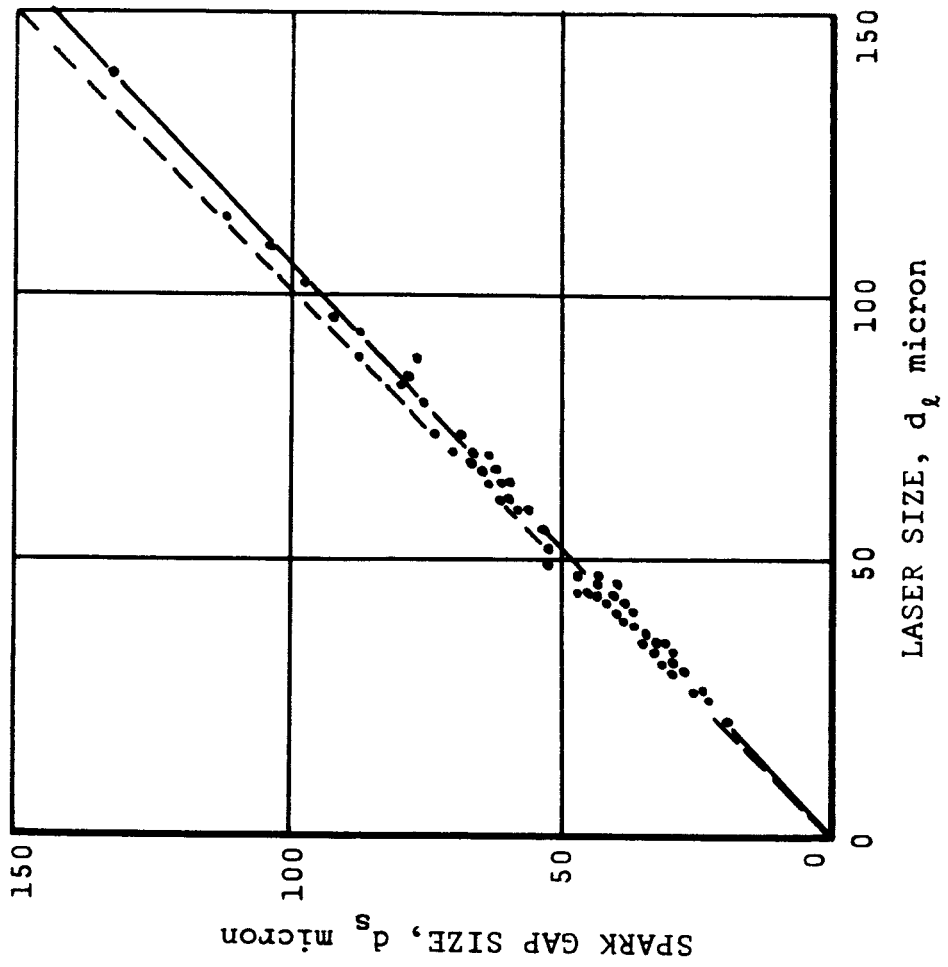
Fig. 10 - Analysis of Size Comparison

These dots show that the images produced by the laser light source usually appear slightly larger than the images produced using the constricted arc light source. In those cases where the image of the drop produced by the constricted arc light source is the larger of the two, it is also the denser of the two. Overexposure then, perhaps makes the drop image appear too large just as under-exposure makes it appear too small. Proper size images should then be possible with the laser KDP cell light source by adjusting the incident light intensity for proper exposure.

CONCLUSIONS

The main conclusions that were reached from this experiment are as follows.

a) Fluorescent dyes in solution, such as Fluorescein Uranin and Rhodamine B Extra, can be excited strongly enough by a single wavelength to be useful in the fluorescent technique for photographing sprays. This is true even though the wavelength is low on the absorption curves of the dyes as $3471 \overset{o}{A}$ is for both these dyes.

b) The duration of the light pulse (20-50 nanosec) from the Q-switched laser tested here is short enough to photograph very high speed drops with no measureable motion blur.

c) The light output of the laser KDP cell combination is adequate to be used for photographing sprays by the fluorescent technique. Such use requires that the light sheet be formed by focusing the laser beam rather than by just blocking out the unwanted portion of the beam. The intensity and amount of $3471 \overset{o}{A}$ light that is available from the ruby laser KDP cell combination is presently limited by the intensity of incident ruby light that the KDP cell can stand. If larger light sheets than the 4 x 5 x .2 mm sheet that is of interest here are required, some way will have to be found to increase the amount of $3471 \overset{o}{A}$ light available from the combination of laser and KDP cell.

d)   The apparent image size of drops lighted by the
laser KDP cell light source is satisfactorily close to the appar-
ent image size of the same drops lighted by the constricted arc
light source. It is felt that apparent image size is a function
of the degree of exposure of the film and that the intensity
of the 3471 $\overset{o}{A}$ light from the laser KDP cell combination can be
controlled so that proper size images will be formed.

e)   The ruby laser KDP cell combination which is available
commercially that was tested here is a very satisfactory light
source for single flash photographing of sprays by the fluor-
escent technique. The question of the usefulness of such
photographs must be answered elsewhere. The use of a laser
light source for timed delay double or multiple exposure photo-
graphing of sprays by the fluorescent technique must await
the development of a laser system that is capable of two or
more timed multiple pulses of ruby light of sufficient power.